EUR 19906 EN

On the Monitoring of Illicit Vessel Discharges

A Reconnaissance Study in the Mediterranean Sea

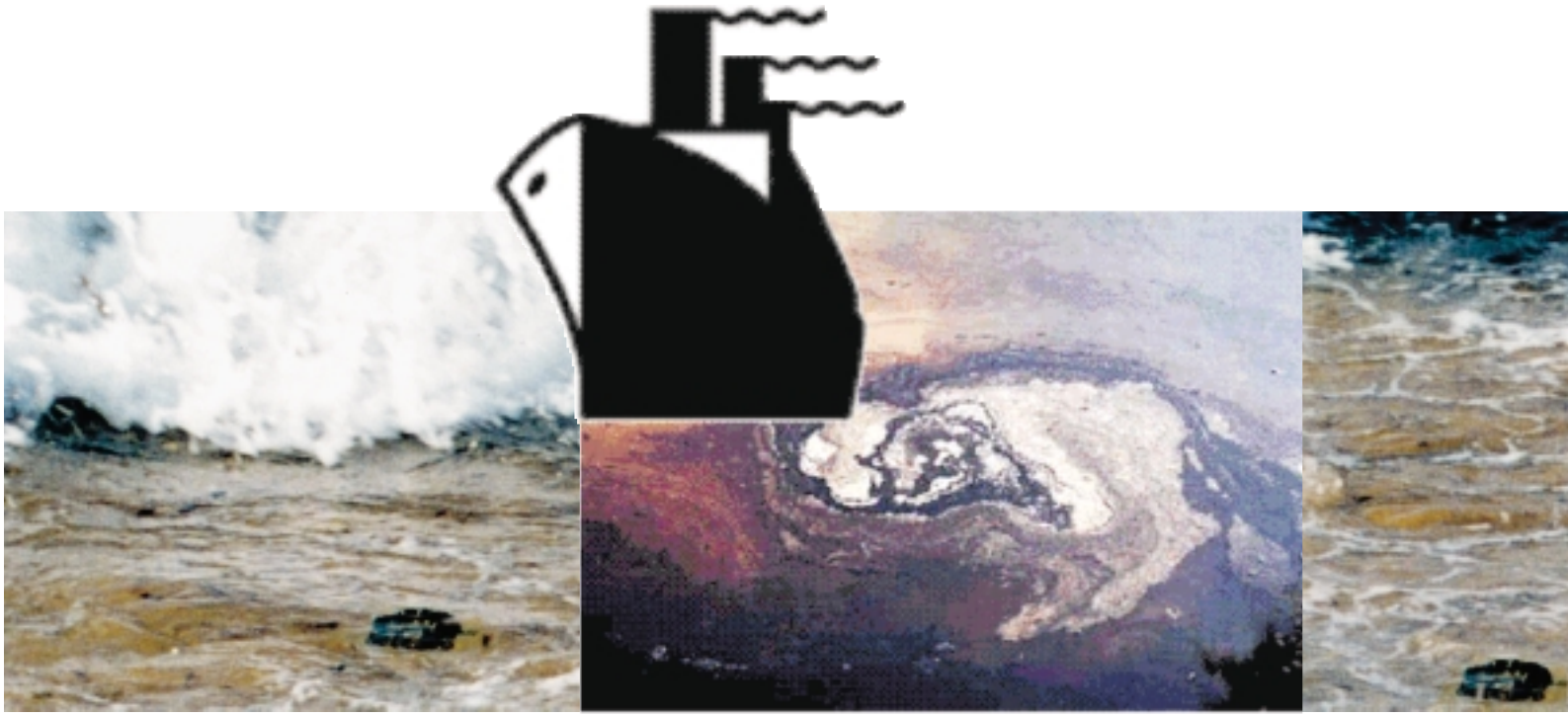

EUROPEAN COMMISSION

EC DG - JOINT RESEARCH CENTRE
Institute for the Protection and
Security of the Citizen
Humanitarian Security Unit

EC DG - ENVIRONMENT
Directorate Environment Quality of
Natural Resources
Civil Protection and Enviro, varies from
few hours to monthsntal Accidents Unit

EUR 19906 EN

On the Monitoring of Illicit Vessel Discharges

A Reconnaissance Study in the Mediterranean Sea

Petros Pavlakis, Dario Tarchi, Alois J. Sieber
EC DG - JOINT RESEARCH CENTRE
Institute for the Protection and Security of the Citizen
Humanitarian Security Unit

In collaboration with

Guido Ferraro and Gilles Vincent
EC DG – ENVIRONMENT
Directorate Environment Quality of Natural Resources
Civil Protection and Environmental Accidents Unit

EUROPEAN COMMISSION

EC DG - JOINT RESEARCH CENTRE
Institute for the Protection and
Security of the Citizen
Humanitarian Security Unit

EC DG - ENVIRONMENT
Directorate Environment Quality of
Natural Resources
Civil Protection and Environmental
Accidents Unit

Printed in Italy

Table of contents

Introduction

Europe is the world's largest market in crude oil imports, representing about one third of the world total. Ninety percent of oil and refined products are transported to and from Europe by sea. Inevitably, some of this oil makes its way into the sea. Whether by accident or normal ship operation, the marine environment is degraded. Accidents resulting in massive spills provide gripping illustrations of the problem of vessel pollution. They are newsworthy and accessible by the mass media, so can affect public opinion and mobilize policy makers to tighten measures for preventing future spills. Such dramatic accidents, however, do not occur frequently, and they represent only a small fraction of the problem of vessel pollution.

Besides accidental pollution, caused by ships in distress, there are three types of routine ship operations, which pollute the sea: ballast water, tank washings and engine room effluent discharges. The first two concern mainly tankers, while the third all types of ships.

Due to these operations large amounts of oil are pumped deliberately from ships every day, along almost all of Europe's coastline. This is the greatest source of marine pollution from ships, and the one that poses an insidious long-term threat to the marine and coastal environment. Of the oil released, the great majority is reported to have come from operational discharges and only a small fraction from accidental spills. Furthermore, while past assessments identified tankers as the main marine polluters with crude oil, recent ones switch the emphasis to fuel oil sludge, engine room waste and bilge water, which are produced by all types of ship.

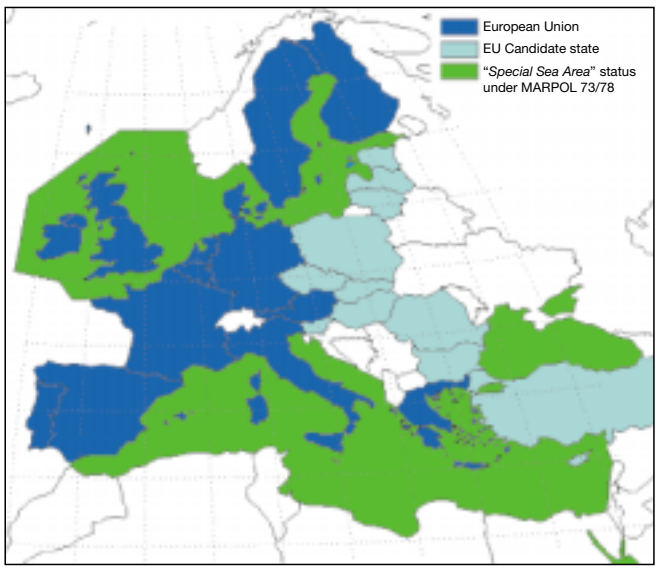

Fig. 1: *Regional seas bordering Europe, which have been declared as Special Areas by the MARPOL 73/78 Convention.*

To reduce time and hence fuel and cost, shipping lanes are often located very close to the coasts. This is particularly the case in European waters, due to the morphological complexity of Europe's coastline. In the Mediterranean, coastal states have in general limited jurisdiction over passing ships flagged by other states. Beyond territorial waters, the role of coastal states is restricted to monitoring, and collecting "*sufficient evidence*" of pollution offences, for reporting to the administrative state of the culprit ship, i.e. its flag state. While the flag states are bound by international law to investigate such reports and punish polluters, what constitutes "*sufficient evidence*" is for them to decide.

Thus the vast bulk of polluting activity takes place just beyond territorial waters. Hence, coastal states have little incentive to undertake costly patrolling of their remote coastal areas, solely for reporting to another state, which also may belong to the black list of "*flags of convenience*". As a consequence, many coastal areas, which may host a wide biodiversity of endangered species, are abandoned to chronic pollution. It is well-known among local people of such areas that when onshore winds are blowing, beaches are dotted for miles by thick, sticky tar balls. Frequently the extent of such damage reaches that of accidental spills, due to accumulation of oil residues augmented by local oceanographic features, such as fronts and eddies.

As the environmental impacts of human activities increase, the rigorous enforcement of international environmental law becomes ever more essential. The answer of the international community to the problem of marine pollution from ships, is the MARPOL 73/78 convention. This takes into account the vital importance of maritime transport, and attempts to strike a balance between the need to protect and preserve the marine environment, and the desire not to make shipping prohibitively expensive.

The MARPOL 73/78 convention, recognizing the specific oceanographic and ecological sensitivity of a number of regional seas, identifies them as "*Special Sea Areas*", (*Annex I, Regulation 10*).

Within these areas the discharge of oil or oily mixtures from ships is completely prohibited, with minor and well defined exceptions. Europe is especially privileged by this regulation, since all its regional seas are now accorded the status of "*Special Sea Area*" (fig. 1).

However, the effectiveness of international environmental agreements depends upon compliance, and for this verification is needed. Verifiable international agreements are more likely to succeed, in both negotiation and implementation. By increasing transparency, so that behaviour and violations are visible to others, verification activities can help to build shared understanding, confidence and norms, which influence behaviour and contribute to regime effectiveness. Verification activities help to assess how effectively a regime has met its goals, and whether changes are needed to improve its effectiveness.

To ensure verification, as well as instigation for compliance, effective capabilities for monitoring and intervention are necessary. In the case of deliberate vessel pollution, monitoring is effective only when supported by continuous airborne surveillance. However, such operations are carried out only over limited geographic areas, since it is not feasible, technically and/or financially, to spread aerial surveillance over the entire breadth of the European waters. As a result, the compliance with the regulations is not applied everywhere with the same care.

As an alternative, spaceborne surveillance can be considered. Synthetic Aperture Radar (SAR) sensors can provide wide-area reconnaissance, and are independent of sunlight or cloud coverage. Satellites equipped with SAR, due to their well proven capability to detect oil spills on the sea surface, as well as to survey large areas of the sea, appear to be ideal for complementing the conventional airborne means. The launch, at the beginning of the last decade, of the first European satellite equipped with SAR, the ERS-1, and later on its successor ERS-2 together with the Canadian RADARSAT-1, made the widespread availability of SAR imagery possible.

In addition, the increasing public anxiety on the detrimental consequences of vessel pollution, and the intention of the *European Commission* to tighten the countermeasures at European level, make the consideration of the spaceborne surveillance possibilities a timely issue. To this end, the *Joint Research Center (JRC)* of the European Commission has initialized regional reconnaissance studies of oil spill occurrences in the European Seas using spaceborne SAR observations.

Aim of this effort is to provide updated information, especially over poorly patrolled regions, in order to assist the Commission services and the European States in assessing on the effectiveness of the existing policies, as well as for optimizing plans of focused patrol and intervention strategies. This document concerns exclusively the problem of monitoring ship discharges with spaceborne SAR and presents the results of a regional reconnaissance study carried out over the entire Mediterranean Sea during 1999. Annexes A, B and C give further technical details on the typical structure and appearance of oil spills from vessel, the possibilities to identify man-made spills in complex image structures as well as an overview of the current scientific knowledge on the topic, respectively.

A case study in the Mediterranean Sea during 1999

The spaceborne SAR surveillance system can give added value to the problem of monitoring marine pollution from ship discharges for the following operational needs:

- **Monitoring of the extent of compliance with regulations, through periodic statistical assessments of spilling events.**
- **Early warning of spilling events, in order to provide rapid mobilization of airborne and/or shipborne platforms for verification.**

We address here these possibilities through the background of a regional study in the Mediterranean Sea. In this Sea the oil transportation is intense, since it is the maritime route to Europe for the oil produced in the Middle East, North Africa and in the Caspian basin. It is estimated (Regional Marine Pollution Emergency Response Centre for the Mediterranean Sea - REMPEC, 1998) that 360 million tones of oil and refined products are transported annually through the Mediterranean Sea representing approximately the 22% of the world total.
However, the Mediterranean is a semi-enclosed sea, connected to the open Ocean solely through the narrow Straits of Gibraltar. Thus, its waters have a long renewal cycle, of up to 90 years. Due to its particular vulnerability to pollution, it was among the first regional seas declared as *Special Areas* by the MARPOL 73/78 convention, three decades ago. In the context also of the *Barcelona Convention*, signed during 1976 by its littoral States including the European Communities, it is required inter alia by the contracting parties to ensure the effective implementation of the international regulations regarding pollution from ships. The emphasis so far has been focused on accidental pollution, which indeed is a visible threat with such intense oil transportation across the region. On the contrary, the pollution problems caused by routine ship operations have not been given sufficient emphasis.
To a large degree this is due to the lack of regional statistics on this activity, since the regular aerial surveillance in the region is limited in comparison to other regional European Seas declared also as *Special Areas*, i.e. the *Baltic Sea* and the *North West European waters*. A first synoptic attempt to assess the oil spill pollution from operational ship discharges in the Mediterranean Sea, was done by the *Joint Research Center (JRC)* of the *European Commission* through spaceborne SAR images (Pavlakis, 1995, Pavlakis et al, 1996). In that study a set of 190 ERS-1 SAR images, acquired along the Mediterranean coastal zone, between 1991-92, were analyzed and yielded a first impression on the extent of the problem. None of the identified spills were found to coincide with a reported accident, while a number of sub-areas were indicated as subjected to higher pressure. Later on, in the frame of the EU funded project CLEAN SEAS, a focused reconnaissance study was carried out over the Gulf of Lion (Gade and Alpers, 1999). Intense local spilling activity was indicated by this study mainly along shipping routes, while the sizes of spills were found to vary from 0.1 km^2 to even more than 56 km^2.

Extent of nonconformity with regulations

The results presented here concern the most recent reconnaissance carried out over the entire Mediterranean region through the analysis of 1600 ERS-1 and 2 SAR images acquired during 1999. The data type used in this study was uncalibrated low-resolution images, since this is the most targeted product for this application. Although these results are preliminary, since they concern only the one quarter of the total number of images acquired during the same period over the region, for a first time they yield a comprehensive picture of the dimension of the problem.
The total area coverage of the analyzed frames is presented on the map of fig. 2. Each square element on this map represents the area covered by a SAR image. In addition, a plot of the spatial repetition density of the analyzed data is presented on the map of fig. 3. As it appears, the density of repetition is highest over the seas surrounding the Italian peninsula. Therefore, the results in terms of spatial distribution are biased towards these areas.
To ensure to the maximum possible degree, that the detected spills were due to man-made activities and not to *look-alike* manifestations of natural phenomena, all the images were interpreted carefully through visual inspection. Each identified spill, was registered on a database, together with information concerning its geographical position, date and time of detection, the spilled area, its average contrast strength, and a vector describing its shape. Within the sample of the 1600 images, 697 were found to

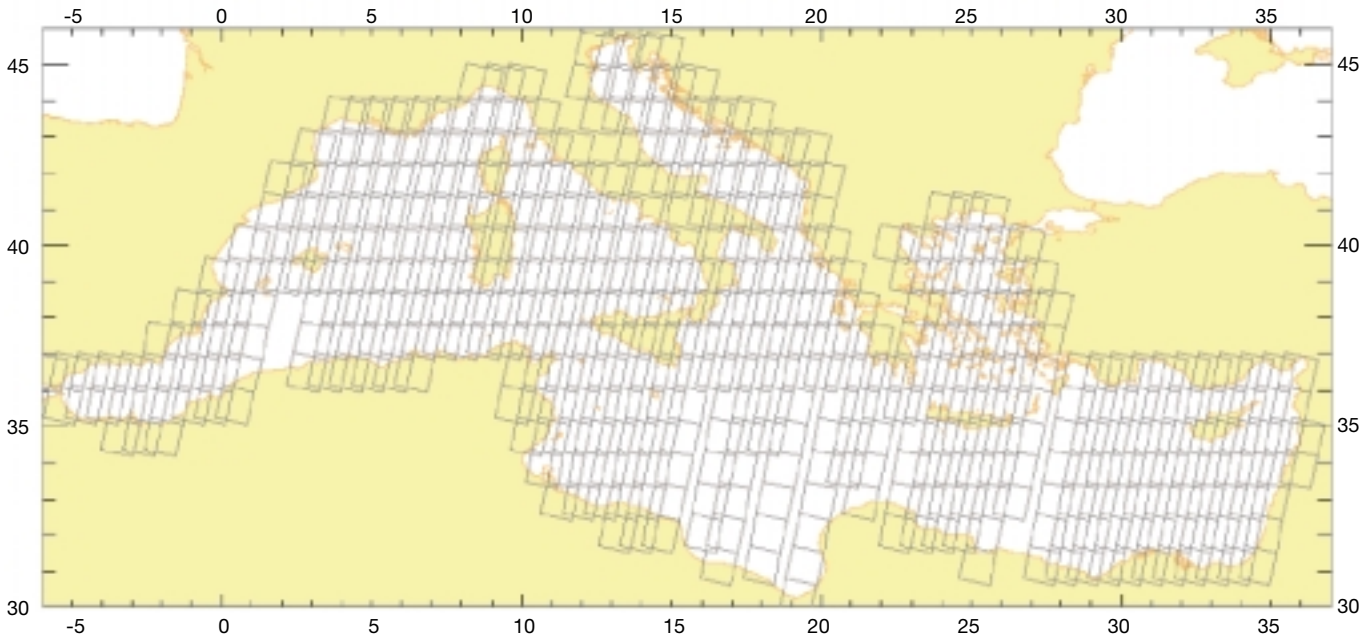

Fig. 2: *The total area coverage of the 1600 ERS-1 and 2 SAR images, which were analyzed in the present study.*

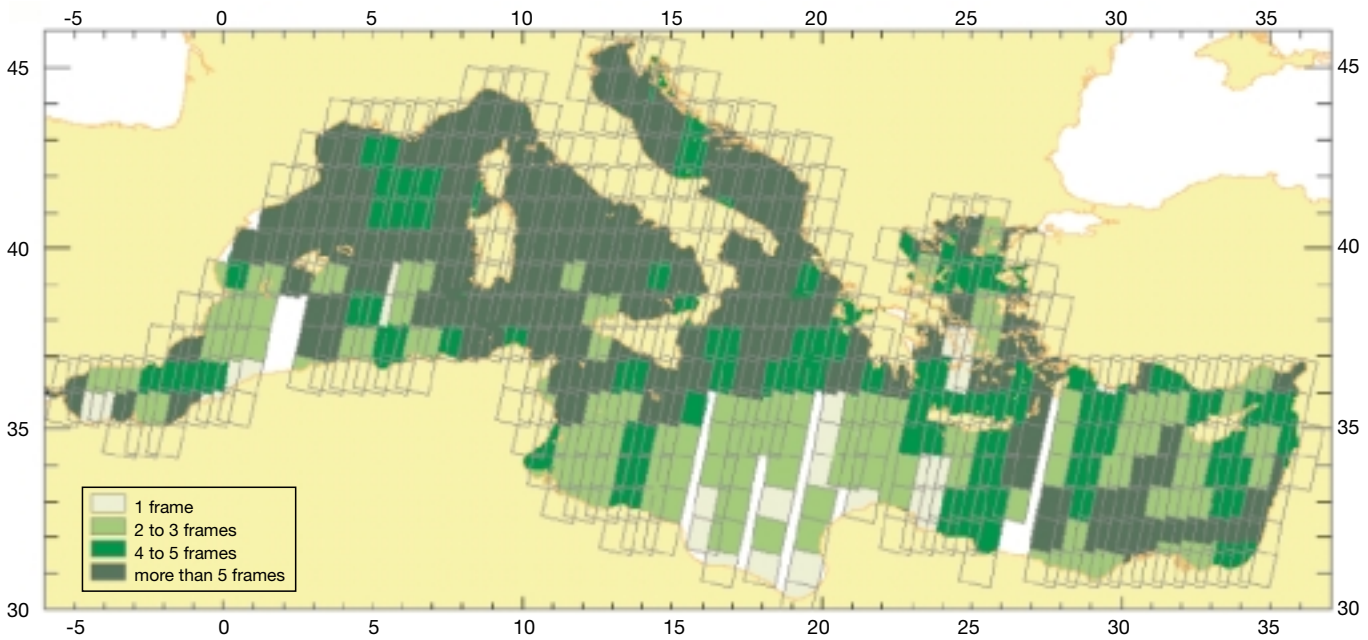

Fig. 3: *Spatial repetition density of the analyzed images.*

contain at least one oil spill signature, representing 44% of the total. However, many images showed more than one spill. As a result, the total number of detected spills was increased to 1638.

A synoptic plot of all the detected spills in the Mediterranean Sea is shown in fig. 4. As it can be observed, enhanced spill concentrations appear along major maritime routes, such as those crossing the Ionian Sea towards the Adriatic Sea, towards the Messina Straits and towards the Sicily Straits. Concentrations along maritime routes appear also in the Ligurian Sea and the Gulf of Lion as well as very close to the East coast of Corsica. In these areas, the spilling appears to be both localized and frequent. All over the region however the spillage show considerable spatial scattering. This is very concerning, since patrol operations are usually focused over known maritime routes.

The total spilled area of the 1638 detected spills was estimated to be 17,141 Km^2. Of interest for the competent authorities, is the amount of oil represented by the spillage. Although an accurate estimation cannot be achieved, since it requires accurate knowledge of the spill thickness that can not be obtained by the SAR sensor alone, some reasonable assumptions can be made that may help

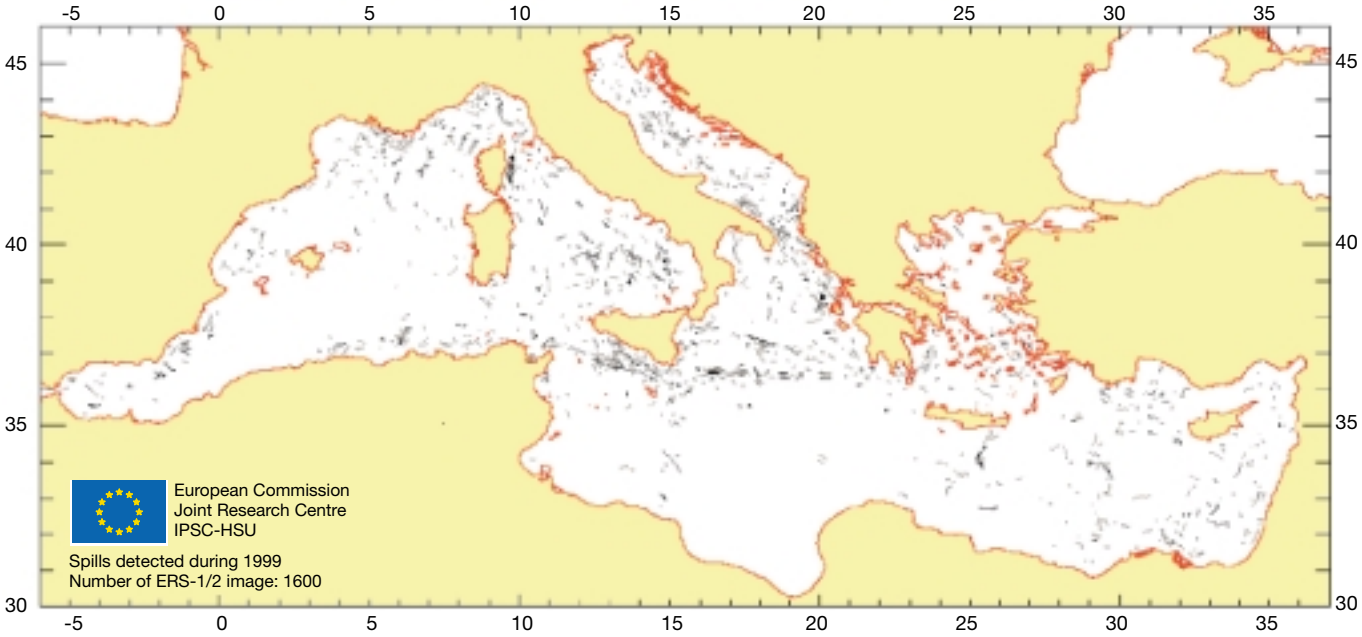

Fig. 4: *Fingerprints of illicit vessel discharges detected on ERS-1 and ERS-2 SAR images, during 1999 in the Mediterranean Sea.*

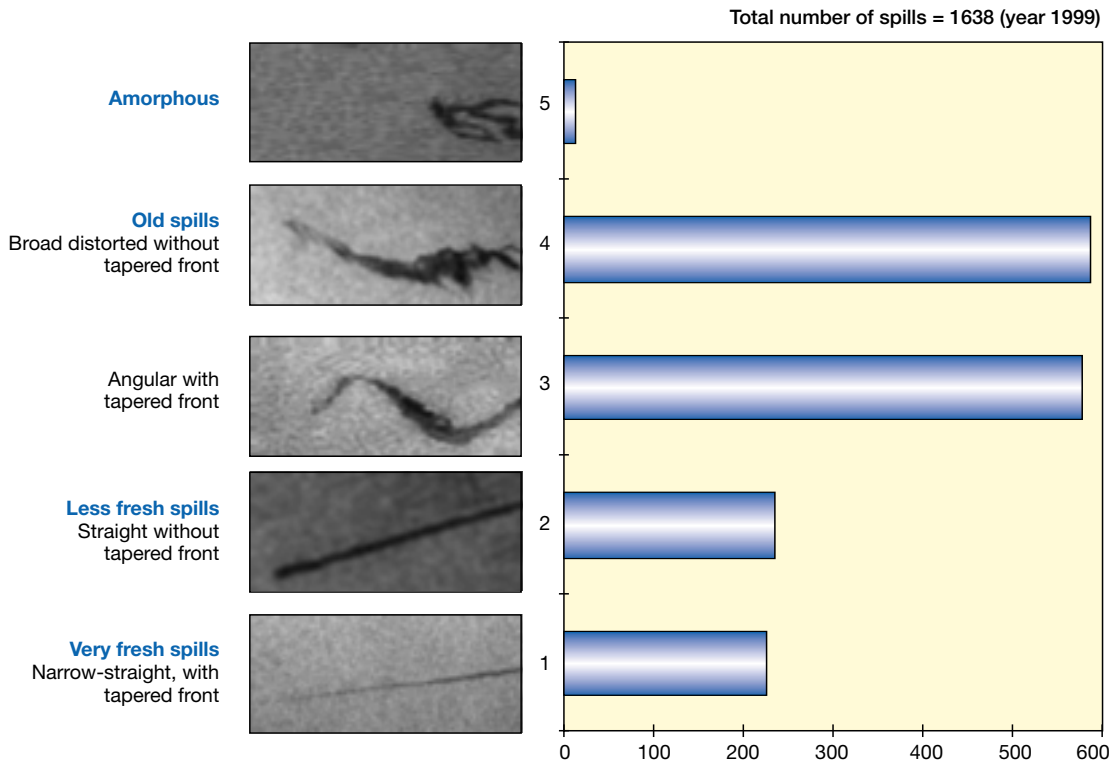

Fig. 5: *Classification of the detected spills in terms of their shapes.*

to obtain an estimate of the spilled amount. For example, Parker and Cormack (1984), after experimental investigations of controlled mineral oil spills in the open sea, concluded that a spill thickness of 0.1 microns was a threshold for imaging it with an airborne SLAR (Side Looking Airborne Radar). Spills of this thickness are considered by operational people as very thin. On an empirical scale of spill thickness against color, these appear as thinner than the barely visible spills. Therefore, making the extreme assumption that all the detected spills in the present study were uniform and of this thickness, we obtain as a minimum amount 1,540 metric tons. To approximate a more realistic number, we may follow as a rule of thumb, the conclusions of Hollinger and Mannella (1984), that the 90% of the oil usually remain in the thicker parts of the spill, which represents only the 10% of its total area. Given such conditions, a revised estimate of 13,858 metric tons is obtained. While the experience may suggest, that even this figure is a rather conservative estimate, it is already four times greater than the average amount spilled in the region by ship accidents (REMPEC, 1998).

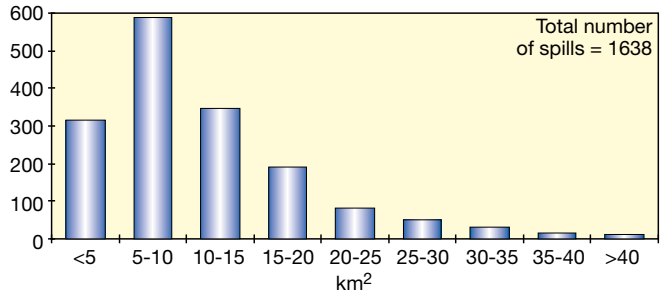

Fig. 6: *Histogram of length sizes of the detected spills.*

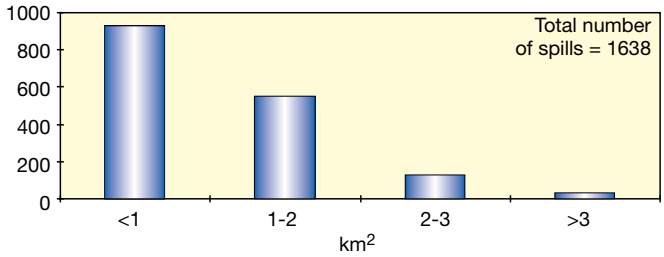

Fig. 7: *Histogram of width sizes of the detected spills.*

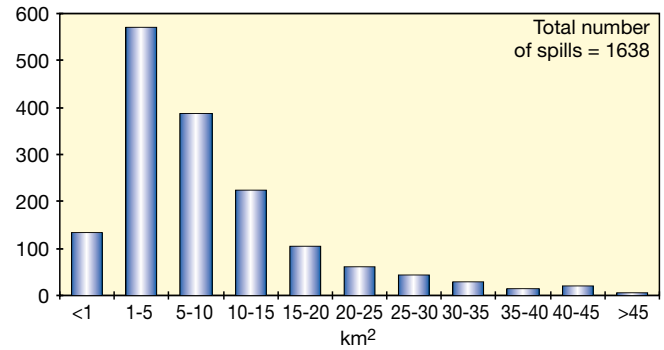

Fig. 8: *Histogram of spilled area sizes of the detected spills.*

In their vast majority the detected spills were of linear shape, either straight or angular. For a first classification, we separated them in 5 categories:
1) narrow straight linear spills, with a tapered front,
2) straight linear spills without tapered front,
3) angular spills with a tapered front,
4) distorted broad spills without tapered front, and
5) amorphous.

The results of this classification are presented in fig. 5. A very small number, about 2% of the total, showed discontinuities. Such spills were classified in accordance to their overall shape using the categories described above. The first two classes indicate fresh spills, and the third category may include also fresh spills resulting from ships changing course. However, this shape may equally indicate spilling over a long time from a stationary ship, during which changes of the wind and the sea currents have occurred. The forth class is considered as old spills in their total.

Statistics of their size variation, in terms of length, maximum width and spilled area, appear in the histograms of figs. 6, 7 and 8 respectively. To better appreciate the significance of these results, consider the regulations of MARPOL 73/78 convention for *Special Areas*. According to this convention (*Regulation 10, Annex I of the Convention*), any discharge of oil or oily mixture from any oil tanker is prohibited, regardless the discharged amount or the distance from the coast. The same ban concerns also engine room waste discharges, from all other ships larger than 400 gt (tons gross tonnage). For ships smaller than 400 gt, excluding oil tankers, discharges are allowed when the oil content of the discharged effluent does not exceed 15 ppm (parts per million). Alternatively, discharges are allowed if all the following conditions are satisfied:

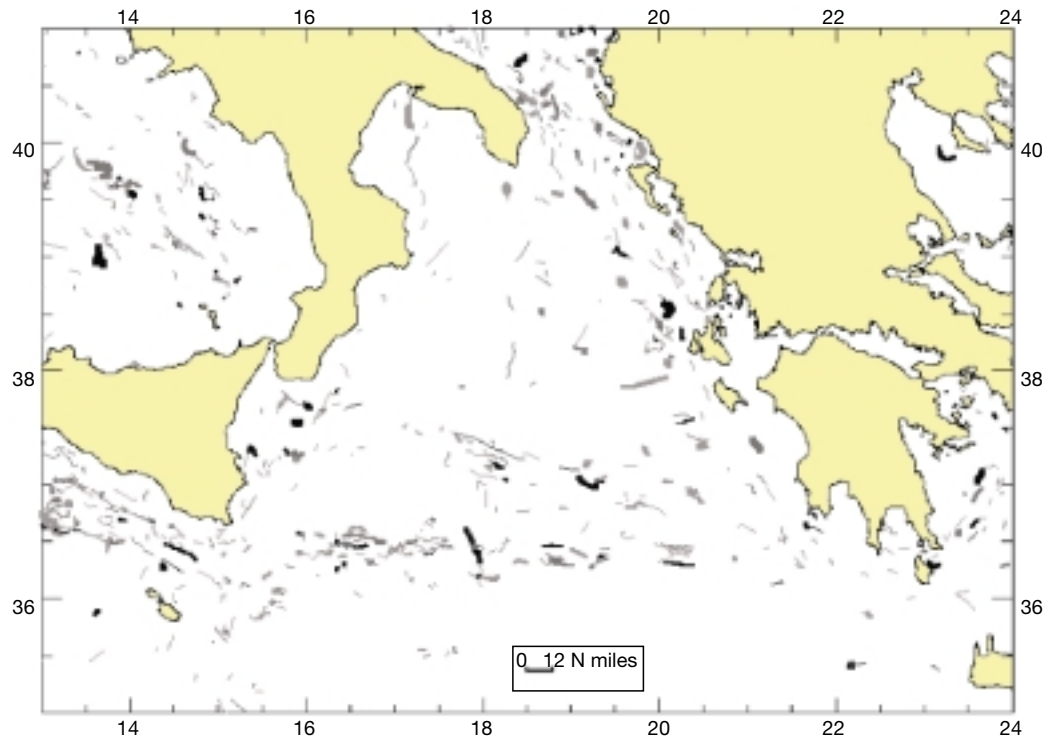

Fig. 9: *Enlarged plot of spills fingertips over the Ionian Sea. The gray scale variations of the spills correspond to classes in terms of radar backscattering contrast strength.*

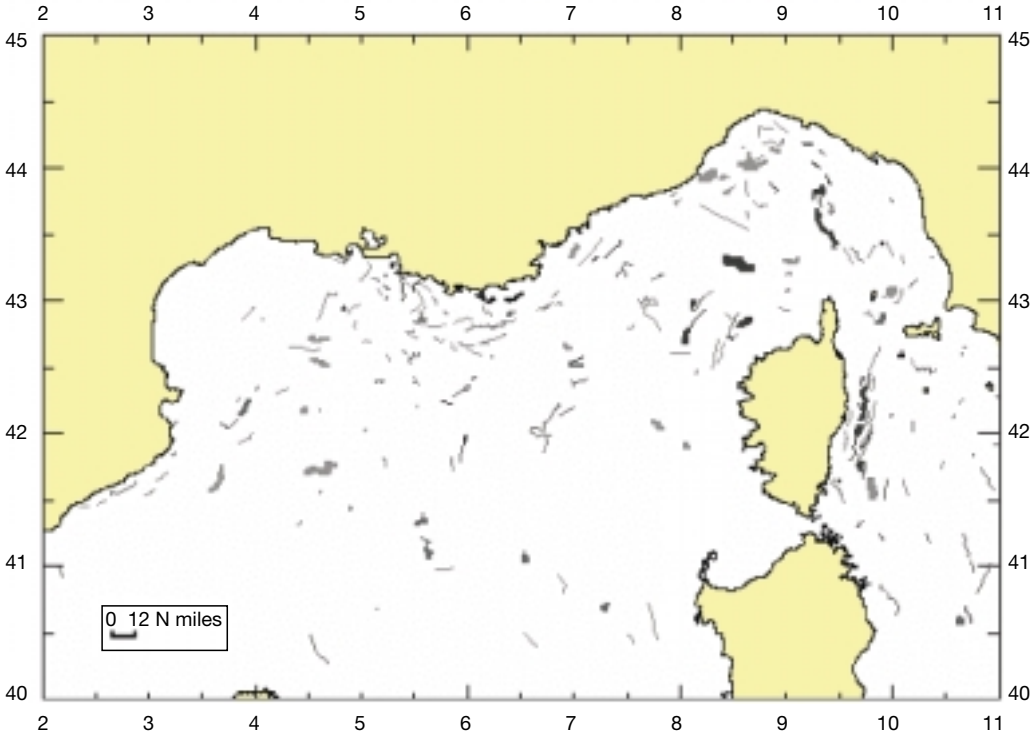

Fig. 10: *Enlarged plot of spills fingertips over the Gulf of Lion and the Ligurian Sea. Note the frequency of spilling along the east-coast of Corsica.*

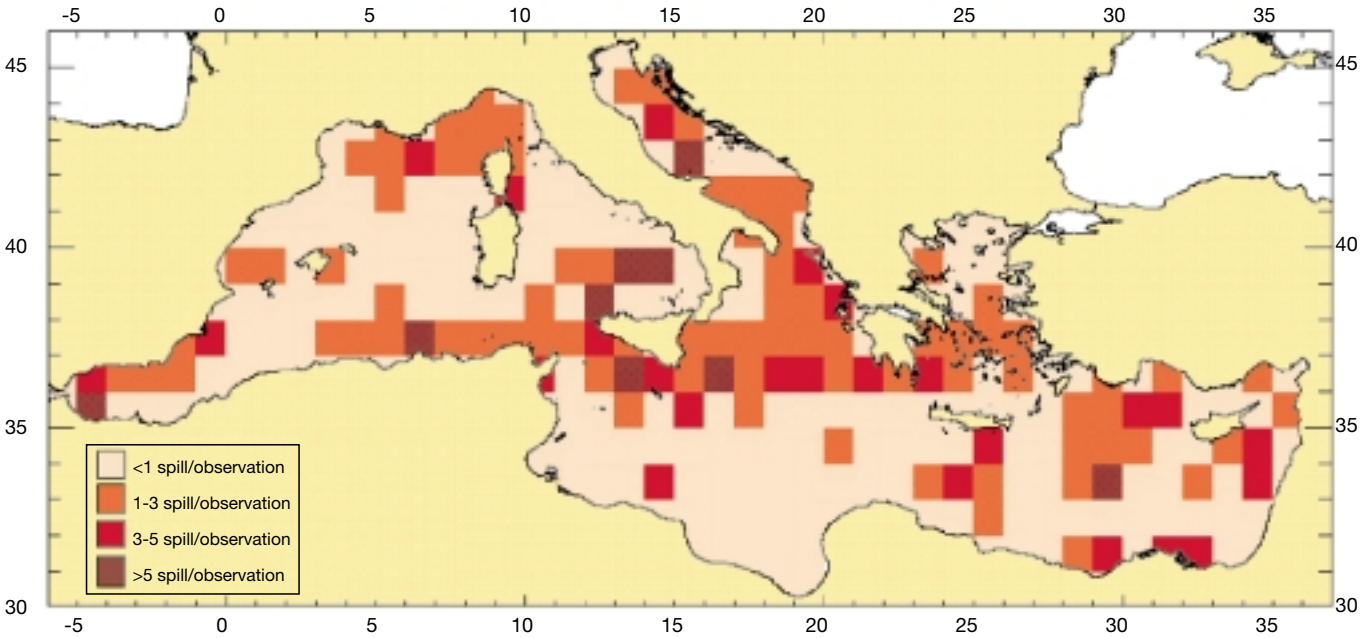

Fig. 11: *Spatial frequency of spilling in terms of number of detected spills within each area element per total number of images covering it (either containing spills or not).*

1) the ship is proceeding en route,
2) the oil content of the discharged effluent is less than 100 ppm,
3) the discharge is made as far as practicable from the land, but in no case less than 12 nautical miles from the nearest coast.

In this context, one may argue that the detected spills cannot be regarded as indicating necessarily unauthorized spilling, since small ships are permitted to discharge. However, the 100 ppm constraint means that even if the full volume of such a small ship is engine effluent (i.e. 400 tons), the amount of oil content within it should not exceed than half a barrel. It is hard to believe that half a barrel of oil is enough to create a spill as large as one square kilometer, which are regularly observed. Therefore, it is highly likely that the vast majority of the detected spills can be regarded as offences. The enlarged part of the map of fig. 4 over the Ionian Sea, presented in fig. 9, illustrates in detail the abundance and broadness of the detected spills. It is constructive also to note that most of the spills

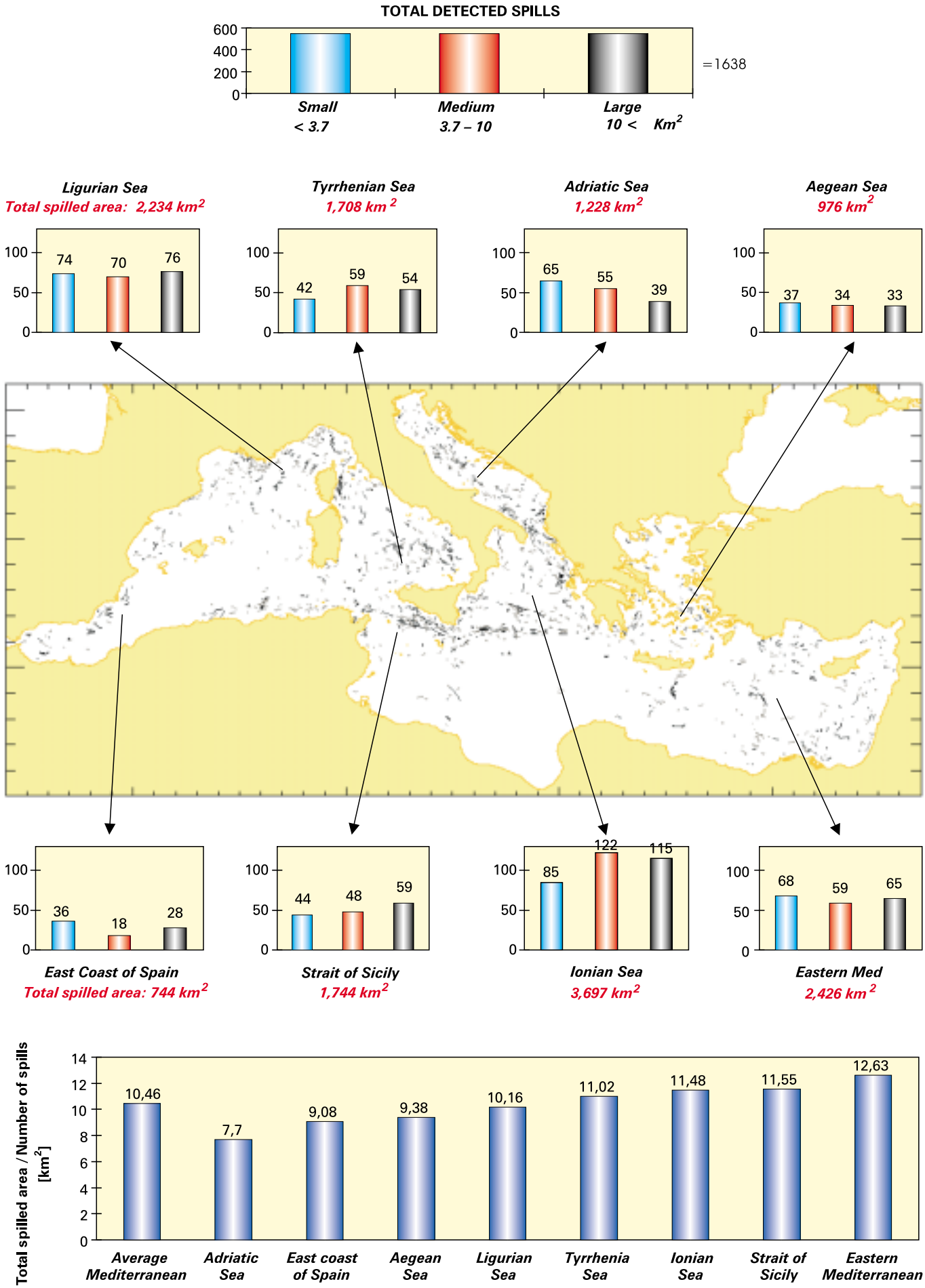

Fig. 12: *Spatial statistics of spill relative-size frequency within sub-areas in the Mediterranean Sea.*

are located beyond the 12 nautical miles limit. In our view, this does not indicate any tendency for compliance, but a deliberate intention to avoid risks of legitimate actions within the area of jurisdiction of the coastal states.
Note, that in the Mediterranean, beyond territorial waters the exclusive right of law enforcement lays with the administrative states of the ships, i.e. their flag states. The role of coastal states is limited to monitoring, collecting evidence and reporting the polluting offences. Perhaps a good example of this is the dark concentration along the East Coast of Corsica (fig. 10). This represents overlapping of many spills of different sizes, on the 12 nautical miles limit boundary.
Although the analyzed images were not uniformly distributed over the Mediterranean region, a first order statistical assessment can be done using the number of detected spills per observation. For this purpose, the region has been divided in square elements of one degree. The ratio of the total detected spills within each element, and the amount of available images (either containing spills or not) covering it, has been computed. A map showing the variation of this ratio is presented in fig. 11.
Based on this map, the region has been divided in to a number of sub-areas where the spilling appears more frequent. From west to east these areas are: *South East Coast of Spain, Gulf of Lion and Ligurian Sea, Central Tyrrhenian Sea, Straits of Sicily, Adriatic Sea, Ionian Sea, South Aegean Sea and Eastern Mediterranean*. Of particular interest, is the relative size of spill signatures within these areas. To investigate this, the total amount of the detected spills in the entire Mediterranean were divided in three equal parts, representing small, medium and large spills. The spill size limits, determined in this way are presented in the top of fig. 12. Consequently the spills detected within each of the aforementioned areas were classified according to these limits. The results are presented around the map in the middle of fig. 12. As it is shown the frequency of spill sizes varies between areas. For example in the Adriatic Sea, small spills are most frequent, which is possibly due to higher traffic of smaller ships in comparison to tankers. On the contrary in the Ionian Sea, Tyhrrenian Sea and the Straits of Sicily, medium to large spills are most prevalent. In particular, the Straits of Sicily is a rather striking case since it concerns a relatively small area. Finally a classification of the sub-areas, in terms of the ratio of total spilled area within them over the number of detected spills is presented at the bottom of fig. 12.

On the age of the detected spills

With current spaceborne SAR capabilities a warning message of oil spilling can be sent to enforcement authorities in 1 and 2 hours. This represents the time required for SAR data acquisition, fast SAR processing, and finally to the image interpretation. Thus, fresh spills represent the most significant signatures, i.e. the categories 1 and 2 of the histogram of fig. 5, together with those of the category 3, which are associated with a bright ship track. Such a summary, as it appears in fig. 13, represents the 40.3% of the total detected spills. Among them 88.2% was associated with ship track (straight or angular), representing 35.5% of the total.
As previously stated, the data used in this study were uncalibrated low-resolution SAR images. Thus many tracks, especially those of small ships, were lost. Even for the fresh spills i.e. the straight linear with tapered front, associated ship tracks were detected only for the 62% of them. Therefore, the 35.5%, which anyway is a considerable percentage,

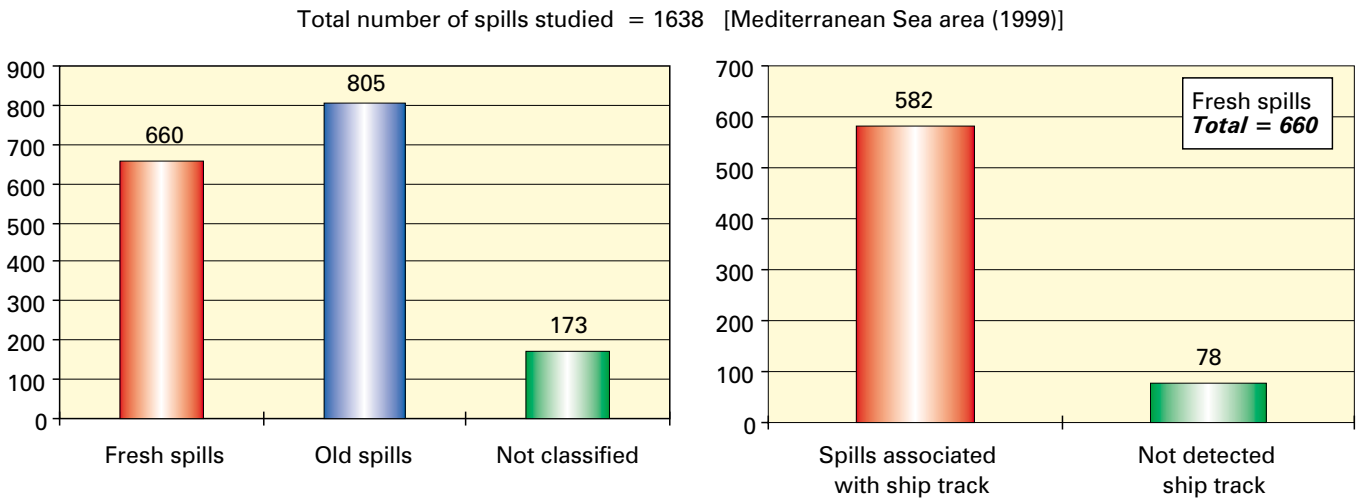

Fig. 13: *Overall assessment on the current operational potential of the spaceborne SAR surveillance in terms of General fresh and old spill classification.*

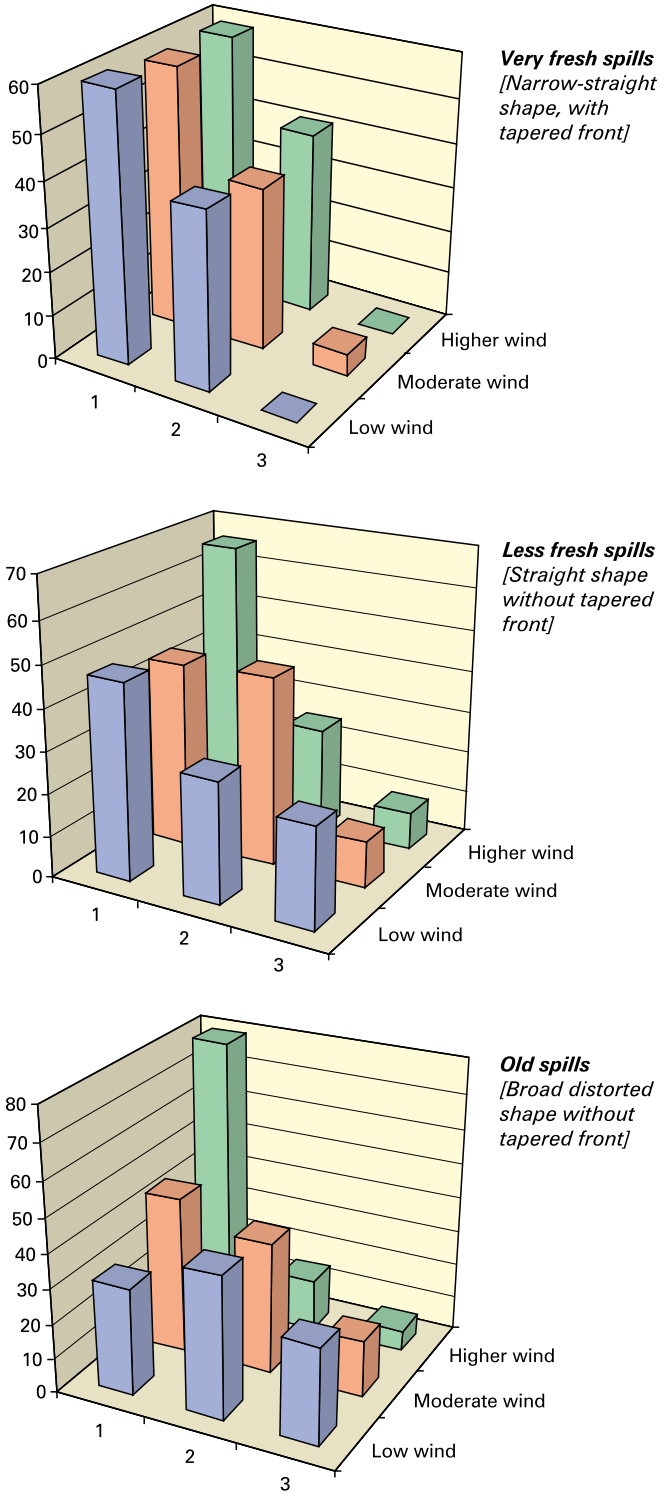

Fig.14: *Histograms of radar backscattering contrast with respect to wind strength level and age of spills (determined in terms of shape criteria). The histograms are normalized along wind strength levels. The contrast levels are as following:* ***1*** *(<4dB),* ***2*** *(4-6dB) and* ***3*** *(>6dB). The wind speed levels are:* ***Low wind*** *(less than 4 m/sec),* ***Moderate wind*** *(4 to 5 m/sec) and* ***Higher wind*** *(above 5 m/sec).*

represents very large ships, i.e. larger than 200 m. By this fact alone, these spills constitute an unquestionable offence since the gross tonnage of such ships by no means is less than 400 tons. However, even for the case of full resolution PRI images (precision images), small ships yield weak radar backscattering signals, and therefore may not be detected especially for above moderate wind speed conditions. As a consequence, the front-tapering and narrowness of a spill appears to be the most significant feature since it may indicate spilling in action at the time of the SAR image acquisition, regardless of the detection of a ship track.

Apart from these features, another interesting indication of freshness of a spill, is the radar backscattering contrast strength. Although the uncalibrated status of the data type did not permit a precise analysis of this aspect, some preliminary considerations were made. For this reason a number of calibrated full resolution PRI images were used, for establishing a correlation scale of the gray level variations of the low-resolution images, against radar backscattering values obtained from the PRIs. Based on this correlation the detected spills were ranked in three levels of contrast:

1) *Low contrast* (less than 4dB),
2) *Intermediate contrast* (between 4 to 6dB),
3) *Strong contrast* (higher than 6db).

Similarly the wind speed was split into three levels, based on the brightness of the surrounding clean sea in the neighborhood of the spill: *Low wind* (less than 4 m/sec), *Moderate wind* (4 to 5 m/sec) and *Higher wind* (above 5 m/sec). For this analysis, we used the spills of the categories 1 (very fresh), 2 (less fresh) and 4 (old spills) of the histogram in figure 5.

The results of this analysis are presented in fig. 14. In order to enable a comprehensive comparison, the frequencies here are normalized along each wind strength level, i.e. the ordinate of the histograms represents percentages. As it can be seen from fig. 14, very fresh spills show weak radar backscattering contrast that is invariant with wind strength. For the spills representing detection a short time after discharge (less fresh spills), there is a tendency of increased contrast, wich appears to be more enhanced at moderate wind speeds. This tendency is also preserved in the older spills but at reduced wind speed. These statistical indications are well in accordance to the rapid increase of the viscosity of the oil, soon after dumping into the sea (Guyomarch and Merlin, 1999). However, as the spill gets older it may becomes more prone to degradation by the sea state.

Conclusions

In general, the appreciation of a new surveillance approach is based on the extent to which it can meet the contemporary necessities of the enforcement of a frame of regulations. However, even in the case that they are not fully met, comprehensive feedback from it, may facilitate the improvement of practices of intervention and enforcement.

Earth observation satellites have helped us to apprehend the vulnerability of our planet and have a measure of the impacts of our activities on the environment we depend upon. We now recognize that as such impacts increase, the rigorous enforcement of international environmental law becomes essential. The work presented in this report, totally based on spaceborne SAR remote-sensing, reveals for the first time the dramatic dimension of shipping pollution in the Mediterranean Sea, not as a result of accidents, but from routine unauthorized operational discharges. The extent of nonconformity, with the international environmental Law in the region, is striking, and calls for more decisive steps forwards.

Several sub-areas of the region appear to face visible threats of chronic pollution and need to receive focused attention. However the detected spills show also considerable spatial scattering, which implies difficulties in monitoring with the limited available airborne conventional means. Thus decisive actions should be taken, for exploiting the maximum possible potential from the spaceborne means. This research has indicated that spaceborne monitoring offers significant advances and is a promising sensor for operating in an early warning role. On the analyzed data a considerable amount of 38.5% spills were considered to represent unquestionably *spilling in action*.

The analysis has also yielded indications, which help to apprehend further the nature of the involved mechanisms in the interactions of the spill with the sea surface roughness, and thus to better understand the variation of the radar backscattering signal from the spilled area. The statistical trends, of the detected spills show that fresher spills yield mostly weak radar backscattering contrast, while the contrast is stronger in the older spills. A dependence on the spill viscosity evolution, appears appropriate for explaining this trend, since it increases rapidly after dumping. Older spills however although viscous, may yield weaker resistance in degradation with increasing sea state.

Annex A

Signatures of spills from ship discharges

From the moment of dumping, the spill formed on the sea changes continuously both in shape and in physico-chemical properties. The processes involved in its evolution, collectively known as *weathering*, are spreading, evaporation, dispersion, emulsification, dissolution, oxidation, sedimentation and biodegradation (Jordan and Payne, 1980). To a certain degree these processes affect the spill contemporarily and even competitively. The time scale however, of their relative importance, varies from few hours to months.

In terms of monitoring ship discharges using Remote Sensing, the most important processes are those with dominating impact on the spill during the first few hours after dumping. Among them the most influential is spreading, that is the rapid expansion of the spill from the point of dumping to all directions in the form of a thin layer. This tendency which is mainly due to gravity and surface tension forces, dominates on the shaping process of the spill during its very early stages. The gravitational spreading force is proportional to the spill thickness, to the thickness gradient, and to the density difference between the water and the dumped oil. All these reduce rapidly with time, thus the spill spreading due to the gravity effect tends quickly to relaxation, and so gives way to that due to surface tension effects. The later is independent of the spill thickness, and results from the difference between the air-water surface tension and the sum of the air-oil and oil-water surface tensions. It depends however on the volatile content of the spill (Fay, 1971), so that when it is removed through evaporation, the spreading due to surface tensional forces tends to termination. Evaporation also is a rapid process and is accelerated with the expansion of the spill, since the area of oil exposed to the air increases.

Therefore, a spill does not spread to infinity but up to a certain limited area, whose extent depends on the amount and the type of the spilled oil. Large amounts of oil will result to large spills, usually within a short time after dumping. On the other hand oils with large volatile and dissoluble in seawater content will result to smaller spills, in comparison to those with less such content, when spilled in the same amounts. The time, a spill requires to reach its maximum breadth, depends on the spreading rate. Many oils tend to spread on the sea surface at about the same rate, even though they possess different viscosities (McAuliffe, 1977). However, highly viscous oils, such as Bunker C, will not spread as rapidly as less viscous ones, especially in cold waters. Furthermore, the spreading is not uniform, since large lateral variations of thickness are frequently observed within a spill, especially of higher viscosity oils. The wind and the sea currents have a strong impact on the lateral variability of the spill thickness. Yet, during its fate in the sea, the oil mixes with surface-active material, which may accelerate differentially the spreading of some parts of its spill. Hollinger and Mannella (1984) showed, through open sea experimental work over controlled spills of different types of oils, that even some hours after discharging ~90% of the oil still remains in its thick parts, which covers only the 10% of its total area extent. Typical spreading rates, computed through the same study, were found to be 0.6 m^2/sec for the spill as a total, while for its thick parts as less as 0.2 m^2/sec.

In the vast majority of cases, the ships discharge their oily effluents en route leaving behind them a linear spill. This *linearity* is the most targeted feature by SAR image interpreters, when tracing spills. In the ideal case, that is discharging in a current free and calm sea, the resulting overall spill geometry will follow the route of the ship. For example discharging along a straight course will result in a straight spill, or a curved/angular spill during maneuvering. If the spill is detected at the time of discharging, its fresher part will have the shape of an elon-

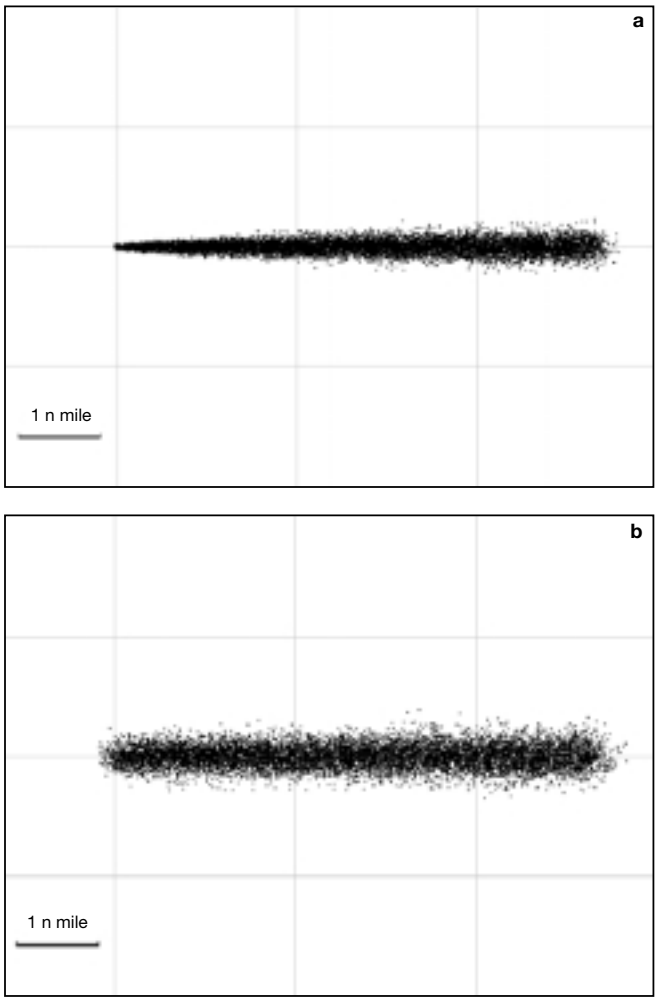

Fig. 15: *Simulations of spills from a ship discharging on a 15knots straight course, an amount of 7 tons of fuel oil. a) Just at the end of discharging, b) 2 hours after discharging. The sea is assumed calm and current free, while the oil is assumed to spread at 0.6 m^2/sec.*

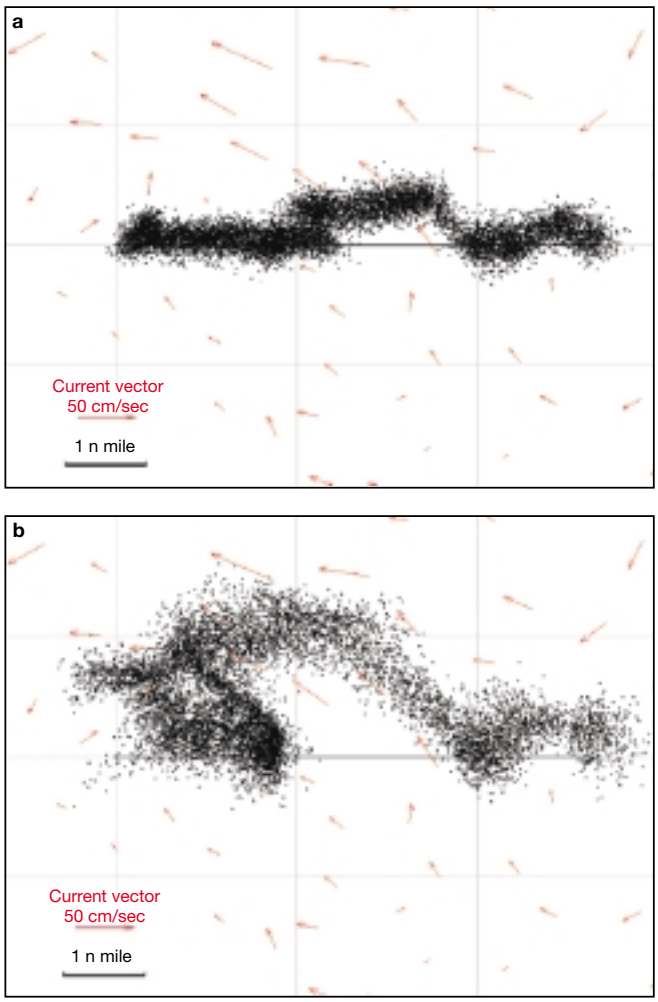

Fig. 16: *Simulations of spill shape distortion by an arbitrary current field a) 1 hour after discharging, b) 3 hours after discharging. The amount of oil, its spreading rate and the speed of the ship during the discharge are the same as in figure 15.*

gated narrow V due to the different spreading time along its length (fig. 15a). However since the spreading is a rapid process, even a short time after the end of discharging, the tapering of its fresher part will disappear. In the simple case of a constant discharging rate along a straight route, the overall shape of the spill will reach that of an elongated parallelogram (fig. 15b).

Even in the presence of wind and current, provided that they are laterally uniform over the wider area within which the spill occurs, and constant during the time of discharging, the initial general shape geometry of the spill will not change significantly during the first few hours. Laterally uniform wind and current fields will deflect only the spill position with respect to the route of the discharging ship.

The situation is different, however when the spill crosses laterally varying surface currents and/or wind fields. In such cases the general geometry of the spill will be distorted. Nevertheless, even in such cases a certain degree of linearity may still be present in the distorted spill shape, aiding thus the interpreter to identify it. However, this depends on the strength of the distorting agents and on the age of the spill (fig. 16). For the typical scales of spills from ship discharges, of greatest important are the sub-mesoscale features of the distorting current and wind fields.

Discharges from a stationary ship in current free and calm sea will result due to spreading, in a broadened spill of a rather rounded shape. The presence of wind and currents however will have a significant impact in this case. Depending on their strength, the resulting spill may take also a linear shape, giving thus the impression, that it is due to dumping from a moving ship. In such cases, accompanied knowledge of the temporal variation of the wind and currents, during the time of spillage, is a key element for understanding the identity of the detected spill (Espedal and Wahl, 1999).

As aforementioned, the wind and the sea currents affect also the internal structure of the spill. The wind in particular has a rather severe effect on it, both directly and indirectly. Directly, because as it drifts the spill, the oil is forced to accumulate in its downwind side, and indirectly, through dynamic processes it generates in the upper sea layer. Most important among them are the near-surface downwind oriented alternating vortices, known as Langmuir circulation (Langmuir, 1934, Thorp, 1995). These vortices tend to concentrate the floating spill along their convergence, while to attenuate it along their divergence. So, the spill splits gradually into streaks, known as feathering, which is usually more apparent in its weaker upwind side.

Annex B

On the detectability of oil spills on SAR images

SAR sensors detect spills on the sea surface indirectly, through the modification they cause on the wind-generated short gravity-capillary waves (Alpers and Huhnerfuss 1989). Spills damp these waves, which at oblique incidence angles are the primary backscattering agents of the radar signals. For this reason, spills are contrasted on the SAR imagery from the surrounding clean sea, as dark patches of reduced backscattering.

Therefore, precondition for detecting oil spills with SAR is the existence of a light wind, sufficient to generate short gravity-capillary waves on the sea surface. The minimum wind speed, referred to as threshold wind speed, depends on the SAR frequency and the angle of incidence. Different microwave bands probe different spectral regions of the gravity-capillary waves, which in turn require different levels of threshold wind speed to be generated. For a C-band SAR, i.e. such as those onboard the ERS-1, ERS-2 and RADARSAT satellites, at least 2 to 3 m/sec wind speed is required for generating gravity-capillary waves, high enough to scatter back detectable microwave energy (Donelan and Pierson, 1987).

On the other extreme, too high wind speed causes the disappearance of the spill from the SAR image. Considering only the wind effect (i.e. assuming that the corresponding sea state is not yet fully developed), at a certain wind speed, the short gravity-capillary waves will receive sufficient energy to counterbalance their energy loss caused by the spill. Under such conditions, spills may be detected at wind speeds as high as 14 m/sec (Pellemans et al, 1995, Pavlakis, 1995). As the sea-state develops however, the increasing turbulence in the upper sea layer may break up the spill and/or sink it, so its effect on the sea surface will be drastically reduced. Hence, with developed sea-state, the upper wind speed limit for spill detection may drop to lower levels. Dedicated open sea experiments (Bern et al 1992, Wahl et al, 1993) indicate, that for wind speeds higher than 10m/sec the detectability of oil spills becomes rather difficult. This depends however on the oil type, as well as on the age and the thickness of the spill.

Extended theoretical and experimental work has been done so far, for understanding the effects involved in the damping of the short gravity-capillary waves by mineral oil spills. However, the responsible mechanisms and their combinations have not yet been clarified. Central aspect of such investigations is the variation of the wave damping strength in a spilled sea surface, as a function of the wavelength of the sea waves. According to the Bragg scattering theory (Wright, 1968, Valenzuela, 1978), at oblique incidence angles, the microwave backscattered intensity is almost proportional to the amplitude of short sea waves, whose wavelength projection, on the radar look direction equals the half of the radar wavelength. Therefore, due to this relation, the wave-damping ratio, between the spilled and clean sea, versus wavelength of sea waves (or wavenumber), can be delineated using multi-frequency scatterometers, and measuring the backscattering at different angles of incidence (Wismann et al, 1993).

According to early investigations of this type, the wave damping effect was deemed as the result of a resonance-type mechanism, directly related to the elastic properties of the floating film of the spill (Singh, at al, 1986, Alpers and Huhnerfuss, 1988). In grater detail, very thin organic films floating on the sea surface, when contracting and expanding under the mechanical motion of the surface waves, give rise to local surface tension gradients, which in turn excite longitudinal waves. When such waves come in resonance with the short gravity-capillary waves, the latter experience maximum damping. This resonance-type theory, known also as *Marangoni damping*, was initially developed for explaining the sea surface smoothness, caused by very thin monomolecular organic films of natural occurrence, i.e. the well known sea slicks (Cini. and Lombardini, 1978, Cini et al, 1983). The consistence however of such slicks is predominantly hydrophilic. Thus, they tend to form on the sea surface uniform monomolecular films, capable to lead to such elastic boundary conditions. Mineral oils on the other hand are predominantly of hydrophobic consistence. So, when spilled into the sea, they spread to form thin layers, but not as thin as those of the monomolecular natural slicks. It can be assumed however (Alpers and Huhnerfuss, 1988), that during their fate in the sea, mineral oils mix with surface-active compounds, formed by photo-oxidation processes and bacterial decomposition. Thus their presence in the mineral oil spill as impurities facilitate the formation of even thinner spill-films, capable to reach locally the necessary elastic boundary conditions for supporting a resonance-type damping mechanism.

To evidence experimentally, such a resonance-type damping mechanism, a relative maximum should be present in the curve of the spilled/clean sea contrast ratio versus wavenumber. Multi-frequency scatterometer data however, obtained through open sea experimental measurements over controlled mineral oil spills, do not reveal clearly such a relative maximum. Instead, the obtained spilled/clean sea contrast ratios appear to increase with wavenumber (Wismann et al, 1998, Gade at al, 1998).

Such results give support to an alternative interpretation, which can be regarded as more suitable to the hydrophobic consistence of mineral oils, and so to their tendency to form thicker spills on the water surface. According to this, the damping effect of the short gravity-capillary waves is linked, in the case of mineral oil spills, to their much higher viscosity, rather than to the elastic properties of their film (Alpers and Huhnerfuss, 1988). This theory is simpler than the resonance-type one, however the complexity of the overall problem remains. This is because, the viscous dissipation does not act alone on the sea surface waves, but coupled with other complicated mechanisms, linear and non-linear; namely: the wind forcing, the wave breaking, and the intrigued exchanges of energy among the waves, when they resonate together in triplets and quartets (Hasselman, 1960, Hasselman, 1968).

However, the viscous-damping consideration has an

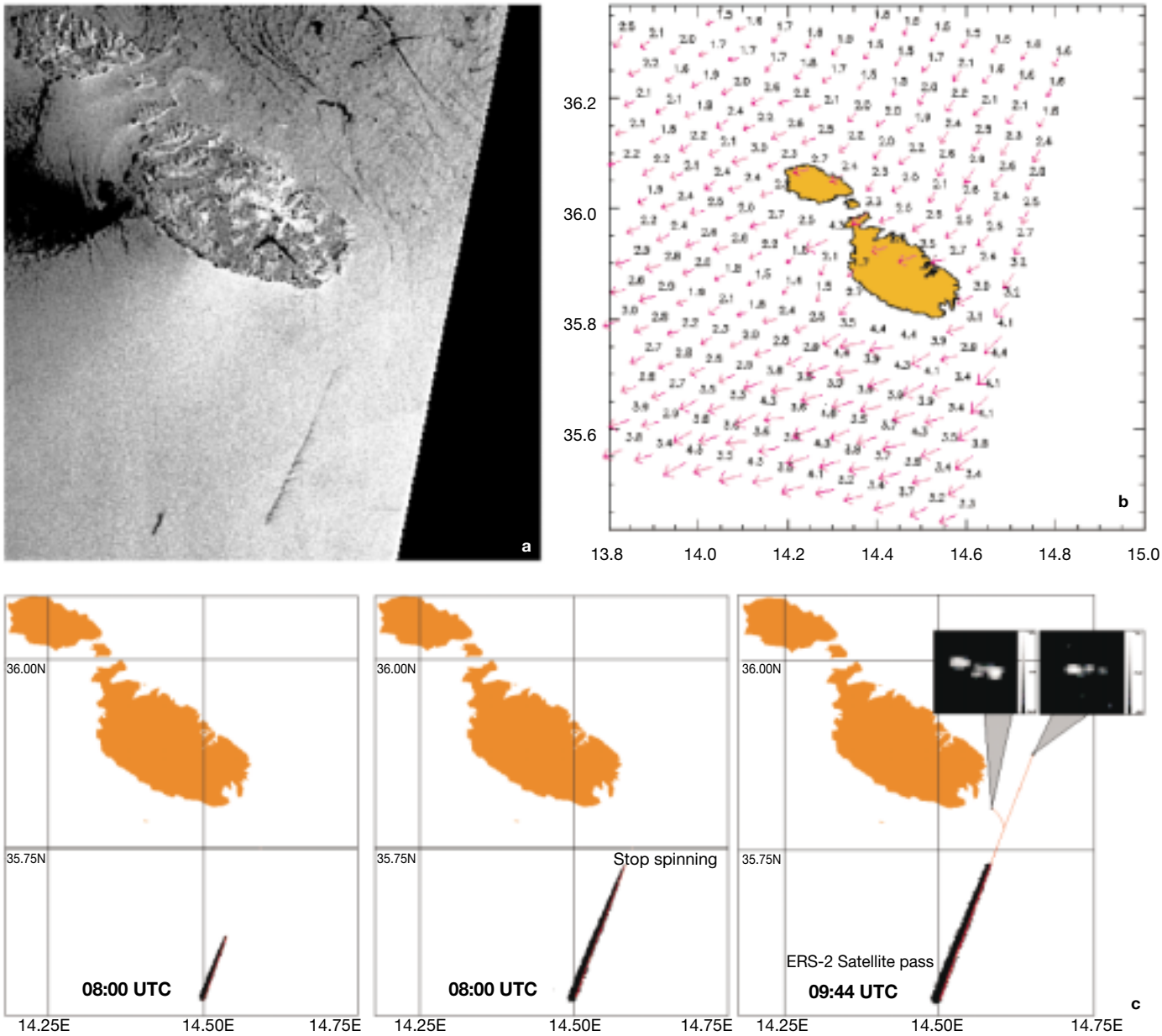

Fig. 17: ***a)*** *SAR image acquired over Malta, showing the signatures of two oil spills (at the bottom of the image). The one on the right shows features, which reveal the wind direction.* ***b)*** *The wind field is retrieved of from the SAR image* ***c)*** *Successive simulations of the releasing scenario of the spill, until to match the imprinted shape. The simulation concludes to a 5 knots ship speed and 0.06 m^3/sec discharging rate. Based on these results the spill can be related to one of the two ship tracks detected in its neighborhood).*

essential practical value, since it explains reasonably, the lateral variability of the radar backscattering contrast within a mineral oil spill, as the result of the lateral variability of thickness and/or viscosity. Indeed, the multi-frequency scatterometer measurements of Wismann et al, (1998) yielded such evidence. In greater detail, higher spilled/clean sea contrast ratios were measured, both over the thicker downwind parts of a mineral oil spill, as well as over spills of higher viscosity oil, in comparison to spills of lower ones. It is obvious that such evidence provide additional grounds for better apprehension of the intrinsic features of the spill fingerprints on the SAR imagery. To this end, since dynamic agents, such as wind, waves and currents influence the spill structure, the center of weight for an essential added value from the spaceborne SAR moves to integrated approaches of interpretation. This is illustrated in the example of figure 17. The SAR image presented here (fig. 17a) shows the signature of a rather fresh oil spill from ship discharging. To reconstruct the history of the spill the wind speed is needed. This can be retrieved by the SAR image itself provided however that its direction is known (Johannessen et al 1998).

The oil spill reveals clearly its leeward thicker side, by its darker edge to the west, which together with the orientation of its banded feathering suggest a wind direction from ENE. With this information the radar backscattering cross section of the surrounding the spill clean sea can be inverted to a high-resolution wind field (fig. 17b). In turn, this wind field helps to simulate the overall shape of the detected spill and through trial and error matching to reconstruct its history, i.e. when its discharging started and ended, as well as the speed of the ship during discharging (fig. 17c). Such additional information will aid to link the spill with ship tracks detected in its neighborhood.

Annex C

The problems in identifying oil spills on SAR images

SAR sensor probes variations of the short gravity-capillary waves. These waves are very sensitive to the highly variable dynamics, of the atmospheric boundary layer and of the upper sea layer. So, the SAR image can be regarded as an instantaneous imprint of the traces of these dynamics on the sea surface. Since their lateral variation are expressed also as gray scale variations on the single band SAR image, they may result to complicated scenerios, posing thus difficulties in the identification of man-made oil spills. To this end the experience of the interpreter and especially its ability to apprehend the nature of the imaged manifestations, becomes a critical factor. As such experience however is not widely available, efforts are in progress, for the development of systems, which may facilitate the detection and identification of man-made oil spills in an automatic or at least in a semi-automatic way (Levett and Sullivan, 1993, Wahl et al, 1994, Calabresi, et al, 1999 among others). A typical display of such a system appears in fig. 18.

The basic functions of such systems can be described briefly as follows:

1) Isolation of all the dark signatures presented on the image, through appropriate threshold and segmentation processing.
2) Extraction of key parameters for each candidate signature, which usually are related to its shape, internal structure and radar backscattering contrast.
3) Test of the extracted parameters against predefined values, which characterize man-made oil spills, usually determined through phenomenological considerations and statistical assessments.
4) Computation of probabilities for each candidate signature on whether it is a man-made oil spill. In more sophisticated approaches also, environmental parameters with impact on the spill shape e.g. the wind speed and currents, are incorporated in the testing step (Espedal and Wahl, 1999).

To a certain degree such systems succeed to discriminate man-made spills, but usually on images with less complex structure. The main reasons of failure with complex images arise usually from the poor automatic parametric description, of key shape features and internal structures of the spill-candidates. Weak radar backscattering contrast of a spill, combined with intense short scale image fabric, such as modulations due to the presence of swell, atmospheric boundary layer rolls, or turbulent wind fluctuations, associated with unstable conditions (i.e. warmer sea surface than the air above) are typical causes. The inherent noise also of the SAR imagery, known as speckle, influences the accuracy of parametric descriptions of spill-candidate signatures. For this reason some filtering of the image is required at a pre-processing stage, for bringing it to an appropriate stage for optimum processing by the detection algorithms. Usually, the selection of pre-processing parameters is based on the decisions of the operator. Therefore, his experience is an important aspect for avoiding biased results.

The presence of extended dark manifestations in the image, due to occurrences other than spills, may not be

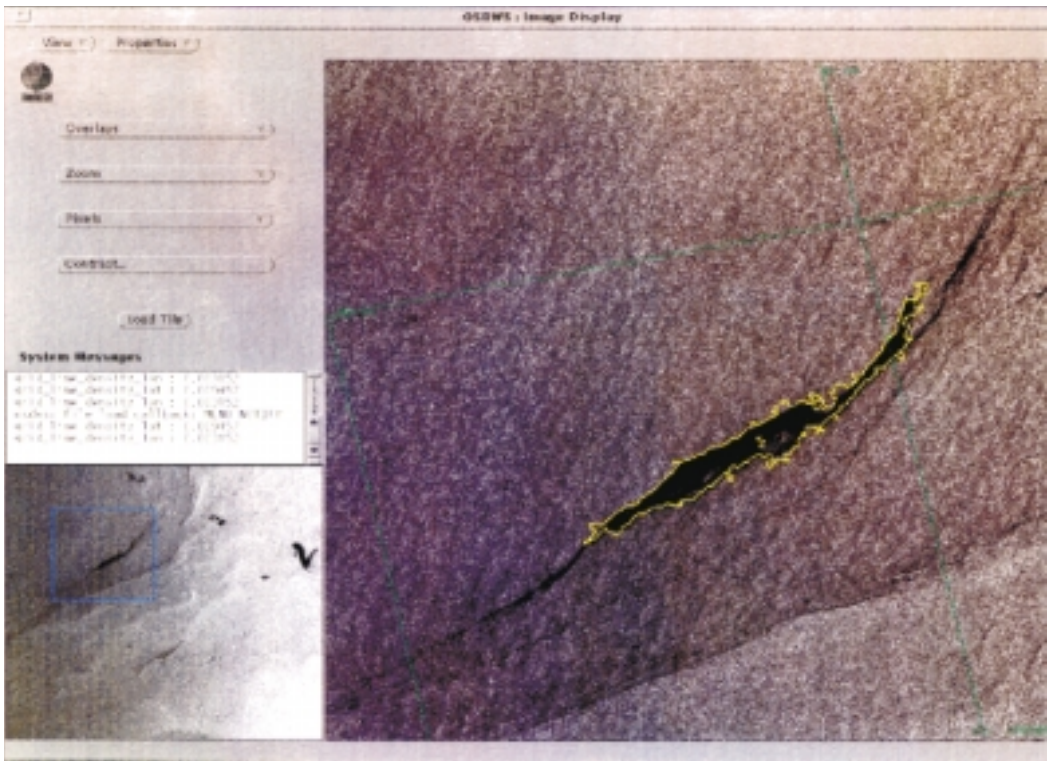

Fig. 18: *The GUI (Graphics Unit Interface) of the OSDWS (Oil Spill Detection Work Station) system, which is used at JRC. (EOS Ltd UK).*

a problem for automatic spill classification, unless they form complex structures of scales comparable to those of man-made spills. Most prone to such complexities are the SAR scenes, acquired under near-threshold wind speed conditions. In such cases, the instantaneous response of short gravity-capillary waves to the variability of the wind, above and below the threshold level, will cause alternations of dark and bright patches on the SAR imagery. Besides, lateral variations of the air-sea stability conditions, may add to the complexity of the SAR scene. Areas of much colder sea than the air above (i.e. highly stable condition), require higher levels of wind speed for short gravity-capillary wave generation (Keller and Plant, 1985, Wu, 1991), thus they may result to dark features at near threshold wind conditions. Rain showers also create short scale turbulence within the uppermost sea layer, which damp the short gravity-capillary waves, so they result to dark SAR signatures (Melsheimer et al, 1996).

Furthermore, dynamics of the upper sea layer, such as lateral current variations may also contribute to confusing manifestations, when they are associated with dark components. Shear boundaries between water masses with different temperature and/or salinity properties, solitary internal waves and surface current variability due to shallow bottom topography are a few of a wide variety of oceanographic features, which may yield SAR signature components, similar to those of oil spills. Their confusing effect increases also when they are associated with natural slicks.

Such slicks, already mentioned, in the previous section occur frequently in the sea, especially under wind speeds less than 5 to 6 m/sec. They are of biological origin and usually form spatial configurations, aligned to the sea current patterns, or tend to accumulate along convergence zones of the current systems, as mineral oil spills too. Since the damping effect they cause on the short gravity capillary waves is to some extent similar to that due to man-made oil spills, they are regarded as one of the major problems in the man-made spill identification process, and have been the subject of extensive investigations. It is worth to mention however, that they are usually dissolved under moderate wind speeds, e.g. above 6 to 7 m/sec, under which, signatures of mineral oil may persist.

In general, complex structures on SAR images are more frequent on those acquired over coastal areas, since many of the aforementioned phenomena are enhanced. The proximity of land also may introduce additional confusing manifestations. These may include, wind shadows behind islands, cold water plumes from river outfalls, cold water upwelling and filaments along shores, plumes of urban discharges, enhanced turbulence along shores etc.

It is obvious that the above constitute a major drawback of the SAR imagery in detecting and identifying oil spills. However, even within such a negative background, spills from ship discharges can be recognized, especially fresh ones. This is because, through the eye of the experienced interpreter, they appear in the most cases, as a rather irrelevant disturbance, within the order of the natural phenomena. Yet, the manifestations of the latter reveal usually their nature, through features of recurrent similarities, which help the interpreter to discriminate them. In this regard, knowledge of local environmental singularities is a substantial aid for this purpose, since most of the recurrent similarities are related to them, e.g. manifestations due to shallow bottom topography. Furthermore, the investigation of such recurrences is a key aspect for "training" also computer-based systems, to do the spill classification process in an automatic way.

To this end, it has to be stressed, that the difficulties posed by the so-called spill *look-alike* manifestations is a partial drawback, and it is not rational to put the spaceborne SAR surveillance in generalized doubt because of it. Beyond areas, which may favor the occurrence of such manifestations, as well as under moderate wind speed conditions, the complexity of SAR images is drastically reduced. So, when a spill is imprinted on it, especially if it is due to ship discharging, it can be identified with a large degree of certainty.

References

Alpers, W. and H. Huhnerfuss, (1988), Radar signatures of oil films floating on the sea surface and the Marangoni effect, J. Geoph. Res., 93, p. 3642-3648.

Alpers, W. and H. Huhnerfuss, (1989)the damping of ocean waves by surface films: A new look at an old problem, J. Geoph. Res., 94, p. 6251-6265.

Berrn, T.-I., T. Wahl, T. Anderssen, and R. Oslen, 1992, Oil Spill Detection using Satellite Based SAR: Experience from a Field Experiment, Proceedings. First ERS-1 Symposium - Space at the Service of our Environment, Cannes, France, 4-6 Nov. 1992, WSA SP-359 (March 1993).

Calabresi, G., F. Del Frate, J. Lichteneger, A. Petrocchi, and P. Trivero, (1999), Neural networks for the oil spill detection using ERS-SAR data, Proceedings, IGARS'99 Hamburg Germany, Vol. I, p. 215-217.

Cini, R. and P.P. Lombardini, (1978), Damping effect of monolayers on surface wave motion in a liquid, J. Colloid Interface Sci., 65, p. 387-389.

Cini, R., P.P. Lombardini, and H. Huhnerfuss, (1983), Remote sensing of marine slicks utilizing their influence on wave spectra, Int. J. Remote Sensing, Vol. 4, No 1, p. 101-110.

Curtis, J.B., Vessel-Source Oil Pollution and MARPOL 73/78: An International Success Story?, 15 Envti. L. 679,692 (1985).

Donelan, M.A. and W.J. Pierson Jr, (1987), Radar scattering and equilibrium ranges in wind-generated waves with application to scatterometry, J. Geophys. Res., 92, 4971-5029.

Espedal, H.A. and Wahl T. (1999), satellite SAR oil spill detection using wind speed history information, Int. J. Remote Sensing, Vol. 20, No 1, 49-65.

Fay, J.A. 1971. Physical processes in the spread of oil on the water surface, p. 467. In Proceedings of 1971 Joint conference on Prevention and control of oil spills, American petroleum Institute, Washington, DC.

Gade, M., and W. Alpers, Using ERS-2 SAR images for routine observation of marine pollution in European coastal waters, Sci. Total Environ., 237-238, 441-448, 1999.

Gade, M., W. Alpers, H. Huhnerfuss, V.R. Wismann, and P.A. Lange (1998), On the Reduction of the radar Backscatter by oceanic Surface Films: Scatterometer Measurements and Their theoretical Interpretation, Remote Sens. Environ. 66 52-70.

Hasselman, K. (1960), Grundegleichungen der Seegangsvoraussage, Schiffstechnik, 7, p. 191-195.

Hasselman, K. (1968), Basic developments in fluid dynamics, Ed. M. Holt, p. 117-182.

Hollinger, J.P. and R.A. Mennella, 1984, Measurements of the distribution and volume of sea-surface oil spills using multifrequency microwave radiometery, In "Remote Sensing for the Control of marine pollution Edited by Jean-Marie Massin NATO Challenges of modern Society Vol. 6 1984Plenum Press.

Huhnerfuss, H.W. Alpers, and F. Witte, (1989), Layers of different thickness on mineral oil spills detected by grey level textures of real aperture radar images, Int. J. Remote Sens. Vol. 10, No 6, p. 1093-1099.

Johannessen J.A., E. Attema, and Y.-L. Desnos (1998), Wind field retrievals from SAR, Earth Obsesvation Quarterly, No 59, June 1998.

Jordan, R.E. and J.R Payne, 1980, Fate and weathering of petroleum spills in the marine environment, Edition Ann Arbore Science - The Butterworth Group, p. 4.

Keller, W.C., and W.J. Plant, (1985), The dependence of X band microwave sea return on atmospheric stability and sea state, J. Geoph. Res., 90, 1019-1029.

Langmuir, I. (1938), Surface motion induced by the wind, Science, 87, 119-123.

Levett, R., and K. Sullivan, (1993), Development of algorithms for automatic detection of oil slicks in SAR images, Res. Rep. No EOS-92/080-RP-002, Earth Observation Systems- EOS Ltd UK.

McAuliffe, C.D., (1977), Dispersal and alteration of oil discharges on a water surface, Proceedings of Symposium: Fate and effects of petroleum hydrocarbons in the marine ecosystems and organisms, November 10-12, 1976, Washington.

Melsheimer, C., W. Alpers, and M. Gade, Investigation of multifrequency/multipolarization radar signatures of rain cells derived from SIR-C/X-SAR data, *Proceed. IGARSS'96*, Lincoln, NE, 1996.

Parker ,H.D. and D. Cormack, (1984), Evaluation of Infrared Line Scan (IRLS) and Side Looking Airborne Radar (SLAR) over controlled oil spills in the North Sea, in Remote Sensing for Control of Marine Pollution, Edited by Jean-Marie Massin, NATO-Chalenges of Modern Society Vol. 6, pp 237-256.

Pavlakis, P. (1995), Investigation of the potential of ERS-1/2 SAR images for monitoring oil spills on the sea surface, Rep. EUR 16351 EN.

Pavlakis, P., A.J. Sieber, and S. Alexandry, (1996), Monitoring oil-spill pollution in the Mediterranean with ERS SAR, Earth Observation Quarterly, Nr 52.

Pedersen, J., L. Seljely, G. D. Strm, O.A. Follum, J.H. Andersen, T. Wahl, and A. Skoelt (1996), Oil spill detection by use of ERS SAR data; from R&D towards pre-operational early warning detection service, Proceedings of the Second ERS Applications Workshop, London, ESA SP-383, ESA Publications Division. The Netherlands.

Pellemans, A.H.J.M., W.G Bos, H. Konings and R.W. van Swol, (1995), Oil Spill Detection on the North Sea using ERS-1 SAR data, Rep. Netherlands Remote Sensing Board (BCRS), Program Bureau, Rijkswaterstaat Survey Department

REMPEC, (1998), Regional Marine Pollution Emergency Response Centre for the Mediterranean Sea, Regional Information System, March 1998.

Siingh, K.P., A.L. Gray, R.K. Hawkins, and R.A. O'Neil, (1986), The influence of surface oil on C-band and K-band ocean backscatter, IEEE Trans. Geosci. Remote Sens., GE-24, p. 738-744.

Thorp, S.A. (1985), Small-scale processes in the upperocean boundary layer, Nature, Vol. 318, 12 Nov. 1985, 519-522.

Valenzuela, G.R. (1978), Theories for the interaction of electromagnetic and oceanic waves - a review, Boundary Layer Meteorol. 13, 61-85.

Vizzari S., Fusco L. A Distributed Oil Spill Monitoring Infrastructure. In: Air & Space Europe. Nr 4/99 Vol 1. Elsevier. 1999

Wahl, T., A. Skely and J. Pedersen, 1994, Practical use of ERS-1 SAR images in oil pollution monitoring. Proceedings of the International Geoscience and Remote Sensing Symposioum (IGARSS 94), Vol. 4. (IEEE), Pisacataway, USA, pp. 1954-1956.

Wismann, V.M. Gade, W. Alpers and H. Huhnerfuss (1998), Radar signatures of marine mineral oil spills measured by an airborne multi-frequency radar, Int. J. Remote. Sens, 19, No 18, 3607-3623.

Wismann, V.R. Theis, W. Alpers and H. Huhnerfuss, (1993), The damping of short gravity-capillary waves by experimental sea slicks measured by a multifrequency microwave scatterometer, Proceedings of OCEANS 93, Victoria, BC, Canada, Vol. II (New York, IEEE), pp. 342-347.

Wright, J.W. (1968), A new model for sea clutter, IEEE Trans. Antennas Propagation, AP-16, 217-223

Wu, J., (1991), Effects of atmospheric stability on ocean ripples: A comparison between optical and microwave measurements, J. Geoph. Res., 96, 7265-7269.